

A Meshless Regularized Integral Equation Method for Laplace Equation in Arbitrary Interior or Exterior Plane Domains

Chein-Shan Liu¹

Abstract: A new *meshless regularized integral equation method* (MRIEM) is developed to solve the interior and exterior Dirichlet problems for the two-dimensional Laplace equation, which consists of three parts: Fourier series expansion, the second kind Fredholm integral equation and an analytically regularized solution of the unknown boundary condition on an *artificial circle*. We find that the new method is powerful even for the problem with complex boundary shape and with random noise disturbing the boundary data.

Keyword: Laplace equation, Meshless method, Regularized integral equation, Artificial circle

1 Introduction

The Dirichlet problem of Laplace equation in plane domain is a classical one. Although analytical solutions have been found for some simple domain with contour like as circle, ellipse, rectangle, etc., in general, for a given plane domain the finding of analytical solutions is not an easy task.

Indeed, the explicit analytical solutions are exceptions, and if one were to choose an arbitrary shape of the domain, the geometric complexity commences and then typically the numerical solution would be required.

Between analytical solutions and numerical solutions for solving the boundary value problems of partial differential equations, there have appeared many semi-analytical solutions in the past several decades. The main reasons for such development could be attributed to that even the most powerful analytical methods are extremely tedious for complicated domain problem, and that even one has an

analytical solution at hand, its numerical results maybe hardly produced. The new method which will be developed here to calculate the Laplace problem in complicated domain is just of this semi-analytical type method. It is in essence an approximation method aiming to find a relatively simple formula for the solution and, at the same time to retain the main feature of exact solution.

The most widely used numerical methods are finite difference method, finite element method and boundary element method (BEM). Despite the popularity of BEM, there are pitfalls to hamper its efficient implementation. To name a few, Lesnic, Elliott and Ingham (1998) have found that the BEM is weak to against the boundary data disturbance which produces unstable solution. Chen, Lin and Chen (2005) have found that the degenerate scale problem and rank deficiency problem may occur for the BEM used in the Laplace equation. The other drawbacks are the requirement of mesh and evaluation of singular integrals, and slow convergence.

For a complicated shape of the domain the above mentioned methods usually require a large number of nodes and elements to match the geometrical shape. In order to overcome these difficulties, the meshless numerical methods were proposed, which are meshes free and only boundary nodes are necessary.

Recently, the meshless local boundary integral equation (LBIE) method [Atluri, Kim and Cho (1999)], and the meshless local Petrov-Galerkin (MLPG) method [Atluri and Shen (2002)] are proposed. Both methods use local weak forms and the integrals can be easily evaluated over regularly shaped domains, like as circles in 2D problems and spheres in 3D problems.

In this paper we are going to propose a new

¹ Department of Mechanical and Mechatronic Engineering, Taiwan Ocean University, Keelung, Taiwan. E-mail: csliau@mail.ntou.edu.tw

meshless method to treat the Dirichlet problem of Laplace equation in the interior or exterior domain:

$$\Delta u(X) = 0, \quad X \in \Omega \text{ or } X \in \mathbb{R}^2/\overline{\Omega}, \quad (1)$$

$$u(P) = h(P), \quad P \in \Gamma, \quad (2)$$

where Ω is a simply connected region in \mathbb{R}^2 with a contour Γ .

It is known that a standard tool to treat the Dirichlet problem is the boundary integral equation [Atkinson (1997); Kress (1989)]. It represents u as a double layer potential:

$$u(X) = \int_{\Gamma} \rho(Y) \frac{\partial}{\partial n_Y} \log |X - Y| dS_Y, \quad X \in \Omega, \quad (3)$$

in which n_Y is the unit normal at $Y \in \Gamma$. The density function ρ satisfies

$$\pi \rho(X) + \int_{\Gamma} \rho(Y) \frac{\partial}{\partial n_Y} \log |X - Y| dS_Y = h(X), \quad X \in \Gamma. \quad (4)$$

If we can parameterize the contour Γ by $\mathbf{r}(t) = (x(t), y(t))$, $t \in [0, 2\pi]$, we can obtain

$$\pi \rho(t) + \int_0^{2\pi} \rho(s) K(t, s) ds = h(t), \quad 0 \leq t \leq 2\pi, \quad (5)$$

where

$$K(t, s) = \begin{cases} \frac{y'(s)[x(s) - x(t)] - x'(s)[y(s) - y(t)]}{[x(s) - x(t)]^2 + [y(s) - y(t)]^2} & t \neq s, \\ \frac{y''(t)x'(t) - x''(t)y'(t)}{2[x'(t)^2 + y'(t)^2]} & t = s. \end{cases} \quad (6)$$

Even the above formulations seem well to introduce a second kind Fredholm integral equation to solve the Dirichlet problem, the kernel function requiring the problem contour to be twice differentiable is a rather stringent restriction in the use of engineering applications. Moreover, the kernel function is not separable, which may introduce certain difficulty to solve the layer density, and

also the solution in terms of double layer potential may include a weak singularity when the field point approaches the boundary. All that makes the computation by using this boundary integral formulation ineffective.

In order to overcome these difficult problems, various numerical methods for solving the Laplace equation are rapidly developed in the last three decades. Recently, Young, Chen and Lee (2005) have proposed a novel meshless method for solving the Laplace equation in arbitrary domain through a rather complicated desingularization technique, Chen, Shen and Chen (2006) utilized the null-field method to calculate the torsion problem with many holes, and in the recent papers by author [Liu (2007a, 2007b, 2007c)], the Laplace equation is solved by the Fredholm integral equation method for the elastic torsion problem and in the doubly connected domain by using the modified indirect Trefftz method and the method of MRIEM.

The other sections of the present paper are arranged as follows. In Section 2 we derive the first kind Fredholm integral equation along a given artificial circle. In Section 3 we consider a direct regularization of the first kind Fredholm integral equation. Then we derive a two-point boundary value problem, which helps us to derive a semi-analytical solution of the second kind Fredholm integral equation in Section 4. In Section 5 we use some examples to test the new method, and then, we give some remarkable conclusions in Section 6.

2 The Fredholm integral equation

In this paper we consider a new meshless method to solve the Dirichlet problem which consists of the Laplace equation and the Dirichlet boundary condition on a non-circular boundary:

$$\Delta u = u_{rr} + \frac{1}{r} u_r + \frac{1}{r^2} u_{\theta\theta} = 0, \quad r < \rho \text{ or } r > \rho, \quad 0 \leq \theta \leq 2\pi, \quad (7)$$

$$u(\rho, \theta) = h(\theta), \quad 0 \leq \theta \leq 2\pi, \quad (8)$$

where $h(\theta)$ is a given function, and $r = \rho(\theta)$ is a given contour describing the boundary shape of

the interior or exterior domain. The contour Γ in the polar coordinates is given by $\Gamma = \{(r, \theta) | r = \rho(\theta), 0 \leq \theta \leq 2\pi\}$.

We replace Eq. (8) by the following boundary condition:

$$u(R_0, \theta) = f(\theta), \quad 0 \leq \theta \leq 2\pi, \quad (9)$$

where $f(\theta)$ is an unknown function to be determined, and R_0 is a given positive constant, such that the disk $D = \{(r, \theta) | r \leq R_0, 0 \leq \theta \leq 2\pi\}$ can cover Ω for the interior problem, or it is inside in the complement of Ω , that is, $D \in \mathbb{R}^2/\overline{\Omega}$ for the exterior problem. Specifically, we may let

$$R_0 \geq \rho_{\max} = \max_{\theta \in [0, 2\pi]} \rho(\theta) \quad (\text{interior problem}), \quad (10)$$

$$R_0 \leq \rho_{\min} = \min_{\theta \in [0, 2\pi]} \rho(\theta) \quad (\text{exterior problem}). \quad (11)$$

Because R_0 is uniquely determined by the contour of the considered problem by Eq. (10) or Eq. (11), we do not worry how to choose R_0 .

The above basic idea is to replace the original boundary condition (8) on a complicated contour by a simpler boundary condition (9) on a specified circle. However, the price we should pay is that we require to derive a new equation to solve $f(\theta)$. If this task can be finished and if the function $f(\theta)$ is available, then the advantage of this replacement is that we have a closed-form solution in terms of the Poisson integral:

$$u(r, \theta) = \pm \frac{1}{2\pi} \int_0^{2\pi} \frac{r^2 - R_0^2}{R_0^2 - 2R_0r \cos(\theta - \xi) + r^2} f(\xi) d\xi. \quad (12)$$

Here, R_0 can be viewed as the radius of an *artificial circle*, and $f(\theta)$ is an unknown function to be determined on this artificial circle. In the above, the positive sign is used for the exterior problem, and conversely the minus sign is used for the interior problem.

By utilizing the technique of separation of variables we can write a Fourier series expansion of

$u(r, \theta)$ satisfying Eqs. (7) and (9):

$$u(r, \theta) = a_0 + \sum_{k=1}^{\infty} \left[a_k \left(\frac{R_0}{r} \right)^{\pm k} \cos k\theta + b_k \left(\frac{R_0}{r} \right)^{\pm k} \sin k\theta \right], \quad (13)$$

where

$$a_0 = \frac{1}{2\pi} \int_0^{2\pi} f(\xi) d\xi, \quad (14)$$

$$a_k = \frac{1}{\pi} \int_0^{2\pi} f(\xi) \cos k\xi d\xi, \quad (15)$$

$$b_k = \frac{1}{\pi} \int_0^{2\pi} f(\xi) \sin k\xi d\xi. \quad (16)$$

Similarly, in Eq. (13) the positive sign before k is used for the exterior problem, and conversely the minus sign before k is used for the interior problem.

By imposing the condition (8) on Eq. (13) we obtain

$$a_0 + \sum_{k=1}^{\infty} \left[a_k \left(\frac{R_0}{\rho} \right)^{\pm k} \cos k\theta + b_k \left(\frac{R_0}{\rho} \right)^{\pm k} \sin k\theta \right] = h(\theta). \quad (17)$$

Substituting Eqs. (14)-(16) into Eq. (17) leads to the first kind Fredholm integral equation:

$$\int_0^{2\pi} K(\theta, \xi) f(\xi) d\xi = h(\theta), \quad (18)$$

where

$$K(\theta, \xi) = \frac{1}{2\pi} + \frac{1}{\pi} \sum_{k=1}^{\infty} \left\{ B^k(\theta) [\cos k\theta \cos k\xi + \sin k\theta \sin k\xi] \right\} \quad (19)$$

is a kernel function, and

$$B(\theta) := \left(\frac{R_0}{\rho(\theta)} \right)^{\pm 1}. \quad (20)$$

Our starting point in Eq. (13) is quite similar to the Trefftz method; however, the Trefftz method is designed to satisfy the governing equation and leaves the unknown coefficients determined by

satisfying the boundary conditions in some manners as by means of the collocation, the least square or the Galerkin method, etc. [Kita and Kamiya (1995)]. Huang and Shaw (1995) have derived an integral representation of the Trefftz method on the so-called embedding surface. However, as remarked by Huang and Shaw (1995) their method is simply an alternative derivation of the Trefftz method. On the other hand, the method of fundamental solutions (MFS), also called the F-Trefftz method, utilizes the fundamental solutions as basis functions to expand the solution. In spite of the apparent differences between the Trefftz method and the MFS, Chen, Wu, Lee and Chen (2007) have proved the equivalence of these two methods for Laplace and biharmonic equations.

Basically, these methods are of the too-early discretized methods, of which the governing equations are discretized into a linear equations system in a rather earlier stage, and not to be continued into the integral equation as we have done in this paper. Therefore, some inherent drawbacks of these methods can be avoided here by the new method, which we would provide a semi-analytical solution of the unknown data on the artificial circle in the next two sections. On the other hand, the usual ill-conditionings appeared in the Trefftz method and the MFS can also be largely improved by our method, as to be shown in Section 5 for the derived linear equations system by numerical examples.

3 Two-point boundary value problem

In order to obtain $f(\theta)$ we have to solve the first kind Fredholm integral equation (18). However this integral equation is known to be ill-posed. We assume that there exists a regularized parameter α , such that Eq. (18) can be regularized by

$$\alpha f(\theta) + \int_0^{2\pi} K(\theta, \xi) f(\xi) d\xi = h(\theta), \quad (21)$$

which is known as one of the second type Fredholm integral equation. The above regularization method to obtain a regularized solution by solving the singularly perturbed operator equation is usually called the Lavrentiev regularization method

[Lavrentiev (1967)].

Up to this point we can remark the differences between Eqs. (21) and (5). In Eq. (5) the kernel function requires the contour curve to be twice differentiable, which is however a rather stringent constraint. But in Eq. (21) the kernel function is well-defined for all contour curves. The kernel function in Eq. (6) is not separable, but the kernel function in Eq. (19) is termwise separable, which makes an easier solution of the integral equation (21) than Eq. (5).

Our method is different from other boundary-type solution procedures, including the BEM, the Trefftz method, the MSF, as well as different type meshless methods. The new method is more easy to handle because it is an integral equation on a given artificial circle, instead of on the contour Γ . As we know in the open literature there has no report to connect the Laplace problem to this type integral equation. About the existence of solution of Eq. (21), Liu (2007a) has given a rigorous proof by using the Fredholm integral theorem.

We assume that the kernel function can be approximated by m terms with

$$K(\theta, \xi) = \frac{1}{2\pi} + \frac{1}{\pi} \sum_{k=1}^m \left\{ B^k(\theta) [\cos k\theta \cos k\xi + \sin k\theta \sin k\xi] \right\}. \quad (22)$$

This assumption is for the convenience of our derivation but is not an essential one. Moreover, the numerical solutions are usually dominated by the first few leading terms.

From Eq. (22) we observe

$$K(\theta, \xi) = \mathbf{P}(\theta) \cdot \mathbf{Q}(\xi), \quad (23)$$

where \mathbf{P} and \mathbf{Q} are $2m+1$ -vectors given by

$$\mathbf{P} := \begin{bmatrix} 1 \\ B \cos \theta \\ B \sin \theta \\ B^2 \cos 2\theta \\ B^2 \sin 2\theta \\ \vdots \\ B^m \cos m\theta \\ B^m \sin m\theta \end{bmatrix}, \quad \mathbf{Q} := \frac{1}{\pi} \begin{bmatrix} \frac{1}{2} \\ \cos \xi \\ \sin \xi \\ \cos 2\xi \\ \sin 2\xi \\ \vdots \\ \cos m\xi \\ \sin m\xi \end{bmatrix}. \quad (24)$$

The dot between \mathbf{P} and \mathbf{Q} denotes the inner product, which is sometimes written as $\mathbf{P}^T\mathbf{Q}$, where the superscript T signifies the transpose.

With the aid of Eq. (23), Eq. (21) can be decomposed as

$$\alpha f(\theta) + \int_0^\theta \mathbf{P}^T(\theta)\mathbf{Q}(\xi)f(\xi)d\xi + \int_\theta^{2\pi} \mathbf{P}^T(\theta)\mathbf{Q}(\xi)f(\xi)d\xi = h(\theta). \quad (25)$$

Let us define

$$\mathbf{u}_1(\theta) := \int_0^\theta f(\xi)\mathbf{Q}(\xi)d\xi, \quad (26)$$

$$\mathbf{u}_2(\theta) := \int_{2\pi}^\theta f(\xi)\mathbf{Q}(\xi)d\xi, \quad (27)$$

and then Eq. (25) can be expressed as

$$\alpha f(\theta) + \mathbf{P}^T(\theta)[\mathbf{u}_1(\theta) - \mathbf{u}_2(\theta)] = h(\theta). \quad (28)$$

Taking the differentials of Eqs. (26) and (27) with respect to θ we obtain

$$\mathbf{u}'_1(\theta) = \mathbf{Q}(\theta)f(\theta), \quad (29)$$

$$\mathbf{u}'_2(\theta) = \mathbf{Q}(\theta)f(\theta). \quad (30)$$

Inserting Eq. (28) for $f(\theta)$ into the above two equations we obtain

$$\alpha\mathbf{u}'_1(\theta) = \mathbf{Q}(\theta)\mathbf{P}^T(\theta)[\mathbf{u}_2(\theta) - \mathbf{u}_1(\theta)] + h(\theta)\mathbf{Q}(\theta), \quad (31)$$

$$\alpha\mathbf{u}'_2(\theta) = \mathbf{Q}(\theta)\mathbf{P}^T(\theta)[\mathbf{u}_2(\theta) - \mathbf{u}_1(\theta)] + h(\theta)\mathbf{Q}(\theta), \quad (32)$$

$$\mathbf{u}_1(0) = \mathbf{0}, \quad \mathbf{u}_2(2\pi) = \mathbf{0}, \quad (33)$$

where the last two conditions follow from Eqs. (26) and (27) immediately. The above equations constitute a two-point boundary value problem.

4 Semi-analytical solution

In this section we will find a semi-analytical solution of $f(\theta)$. From Eqs. (29) and (30) it can be seen that $\mathbf{u}'_1 = \mathbf{u}'_2$, which means that

$$\mathbf{u}_1 = \mathbf{u}_2 + \mathbf{c}, \quad (34)$$

where \mathbf{c} is a constant vector to be determined. By using the final condition in Eq. (33) we find that

$$\mathbf{u}_1(2\pi) = \mathbf{u}_2(2\pi) + \mathbf{c} = \mathbf{c}. \quad (35)$$

From Eqs. (26) and (35) it follows that

$$\mathbf{c} = \int_0^{2\pi} f(\xi)\mathbf{Q}(\xi)d\xi. \quad (36)$$

The mathematical meaning of \mathbf{c} is that it is a vector of the Fourier coefficients of the unknown function $f(\theta)$.

Substituting Eq. (34) into Eq. (31) we have

$$\alpha\mathbf{u}'_1(\theta) = -\mathbf{Q}(\theta)\mathbf{P}^T(\theta)\mathbf{c} + h(\theta)\mathbf{Q}(\theta). \quad (37)$$

Integrating and using the initial condition in Eq. (33) it follows that

$$\mathbf{u}_1(\theta) = \frac{-1}{\alpha} \int_0^\theta \mathbf{Q}(\xi)\mathbf{P}^T(\xi)d\xi \mathbf{c} + \frac{1}{\alpha} \int_0^\theta h(\xi)\mathbf{Q}(\xi)d\xi. \quad (38)$$

Taking $\theta = 2\pi$ in the above equation and imposing the condition (35) one obtains a linear equation for \mathbf{c} :

$$\mathbf{R}\mathbf{c} = \mathbf{d}, \quad (39)$$

where

$$\mathbf{R} := \alpha\mathbf{I}_{2m+1} + \int_0^{2\pi} \mathbf{Q}(\xi)\mathbf{P}^T(\xi)d\xi, \quad (40)$$

$$\mathbf{d} := \int_0^{2\pi} h(\xi)\mathbf{Q}(\xi)d\xi. \quad (41)$$

Corresponding to \mathbf{c} , \mathbf{d} is a vector of the Fourier coefficients of the given boundary function $h(\theta)$.

Then, the conjugate gradient method is used to solve the following normal equation for \mathbf{c} :

$$\mathbf{A}\mathbf{c} = \mathbf{b}, \quad (42)$$

where

$$\mathbf{A} := \mathbf{R}^T\mathbf{R}, \quad \mathbf{b} := \mathbf{R}^T \int_0^{2\pi} h(\xi)\mathbf{Q}(\xi)d\xi. \quad (43)$$

Eq. (36) indicates that \mathbf{c} is a vector of the Fourier coefficients of the function $f(\theta)$, and then we can

express the solution of u in terms of \mathbf{c} explicitly by

$$u(r, \theta) = c_1 + \sum_{k=1}^m \left[c_{2k} \left(\frac{R_0}{r} \right)^{\pm k} \cos k\theta + c_{2k+1} \left(\frac{R_0}{r} \right)^{\pm k} \sin k\theta \right], \quad (44)$$

where (c_1, \dots, c_{2m+1}) are the components of \mathbf{c} . Because in these processes we do not require any domain or surface meshing, the new meshless method would be very convenient for engineering applications in the computation of complex boundary shape problems.

On the other hand, from Eqs. (28) and (34) we have

$$\alpha f(\theta) = h(\theta) - \mathbf{P}(\theta) \cdot \mathbf{c}. \quad (45)$$

Inserting the solved \mathbf{c} into the above equation we obtain a semi-analytical solution of the second kind Fredholm integral equation (21).

For the later use in numerical example we consider a special case with the boundary curve being a circle, that is, $\rho = \rho_0$ with ρ_0 a give positive constant number. For this case we can select the artificial circle to be the same circle, such that $R_0 = \rho_0$ and $B = 1$ by Eq. (20). For this case \mathbf{P} and \mathbf{Q} are orthogonal, and thus we have

$$\mathbf{c} = \frac{1}{1 + \alpha} \mathbf{d} \quad (46)$$

by Eqs. (39) and (40). Thus, the solution of u can be simplified to

$$u(r, \theta) = \frac{d_1}{1 + \alpha} + \sum_{k=1}^m \left[\frac{d_{2k}}{1 + \alpha} \left(\frac{R_0}{r} \right)^{\pm k} \cos k\theta + \frac{d_{2k+1}}{1 + \alpha} \left(\frac{R_0}{r} \right)^{\pm k} \sin k\theta \right], \quad (47)$$

where (d_1, \dots, d_{2m+1}) are the components of \mathbf{d} .

5 Numerical examples

Before embarking the numerical study of the new method, we are concerned with the stability of

MRIEM, in the case when the boundary data are contaminated by random noise, which is investigated by adding the different levels of random noise on the boundary data. We use the function RANDOM_NUMBER given in Fortran to generate the noisy data $R(i)$, where $R(i)$ are random numbers in $[-1, 1]$. Hence we use the simulated noisy data given by

$$\hat{h}(\theta_i) = h(\theta_i) + \varepsilon R(i), \quad (48)$$

where $\theta_i = 2i\pi/n_b$, $i = 0, 1, \dots, n_b$, and ε is defined as

$$\varepsilon = \max |h(\theta)| \times \frac{s}{100}, \quad (49)$$

where s is the percentage of additive noise on the data.

5.1 Example 1 (exterior problem)

In this example we investigate a discontinuous boundary condition on the unit circle:

$$h(\theta) = \begin{cases} 1 & 0 \leq \theta < \pi, \\ -1 & \pi \leq \theta < 2\pi. \end{cases} \quad (50)$$

For this example an analytical solution is given by

$$u(x, y) = \frac{2}{\pi} \arctan \left(\frac{2y}{x^2 + y^2 - 1} \right). \quad (51)$$

We have applied the new method in Eq. (47) to this example by fixing $R_0 = 1$, $m = 20$ and $\alpha = 10^{-10}$. In Fig. 1(a) we compare the exact solution with numerical solutions with $s = 0, 5$ along a circle with radius 2.5. It can be seen that the numerical solutions are very close to the exact solution. Furthermore, the numerical errors were plotted in Fig. 1(b), of which it can be seen that the present method is very robust to against the noise, whose level was taken up to 5% ($s = 5$), and the numerical error is still smaller than 0.02. In Fig. 1(c) we also compare the numerical and exact contour levels of $u = -0.3, -0.2, -0.1, 0.2, 0.3, 0.4$. The differences of numerical and exact results are very small.

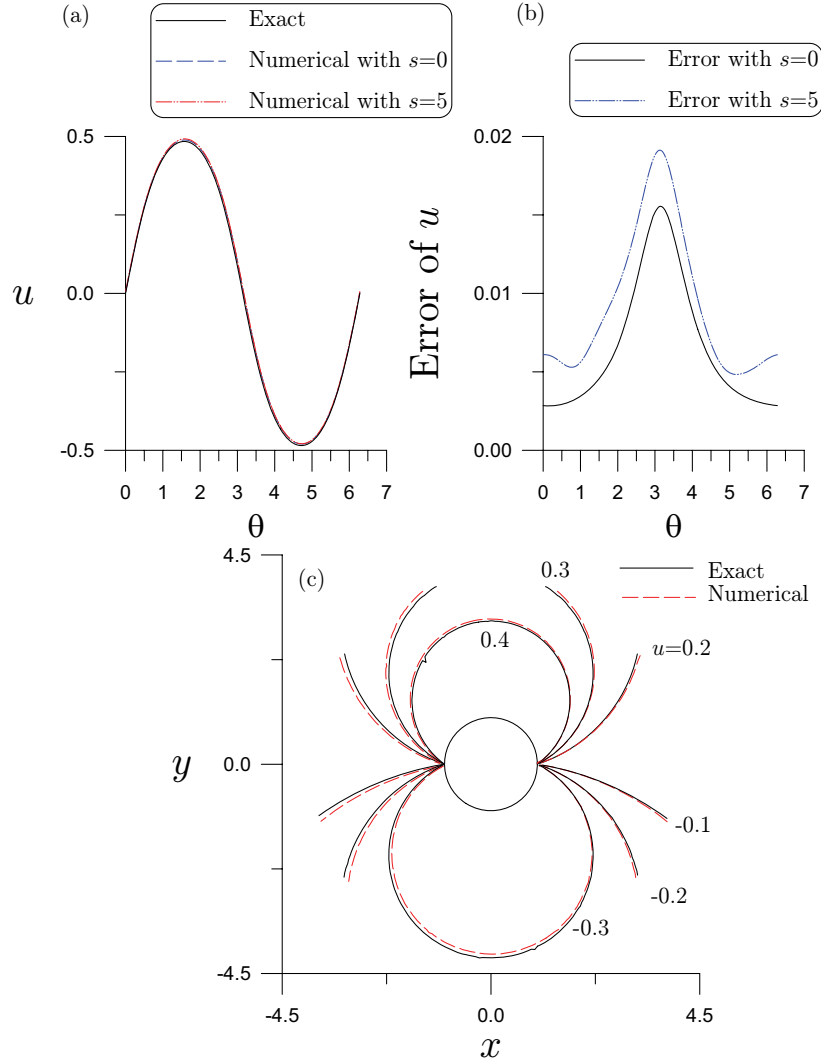


Figure 1: For Example 1 the comparisons of exact solution and numerical solutions with noise $s = 0, 5$ are made in (a), the numerical errors are plotted in (b), and in (c) several contour levels of potential are compared.

5.2 Example 2 (exterior problem)

In this example we consider a complex epitrochoid boundary shape

$$\rho(\theta) = \sqrt{(a+b)^2 + 1 - 2(a+b)\cos(a\theta/b)}, \tag{52}$$

$$x(\theta) = \rho \cos \theta, \quad y(\theta) = \rho \sin \theta \tag{53}$$

with $a = 3$ and $b = 1$. It is known that the solution of Eq. (42) controls the accuracy of numerical solution. In order to identify its well-posedness we plot the condition number of \mathbf{A} with respect to m

and R_0 in Fig. 2, which is defined by

$$\text{Cond}(\mathbf{A}) = \|\mathbf{A}\| \|\mathbf{A}^{-1}\|. \tag{54}$$

The norm for \mathbf{A} is the Frobenius norm. When m increases the condition number also increases as shown in Fig. 2(a); however, even with $m = 30$ the condition number is still smaller than 300. The condition number decreases with respect to R_0 as shown in Fig. 2(b), which indicates that for this case with $R_0 = \rho_{\min} = 3$ the condition number getting the smallest value.

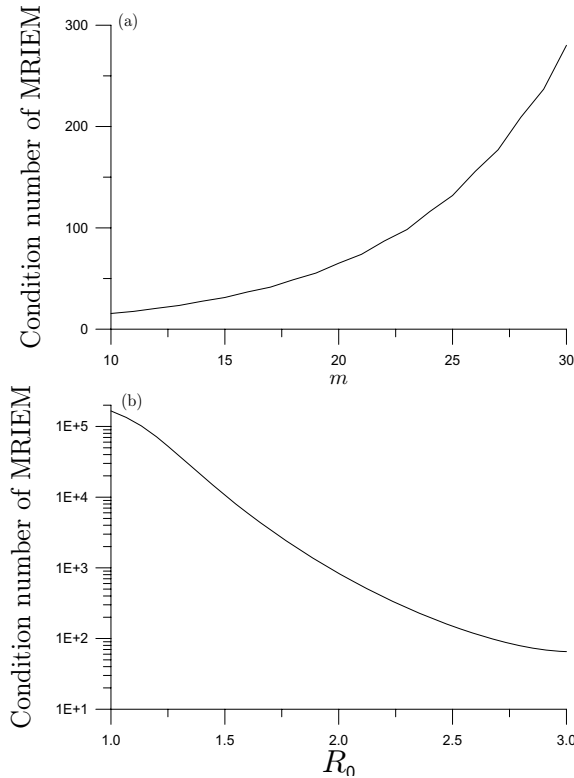


Figure 2: For Example 2 we plotting the condition number with respect to m in (a) and R_0 in (b).

The analytical solution is supposed to be

$$u(x,y) = \exp\left(\frac{x}{x^2+y^2}\right) \cos\left(\frac{y}{x^2+y^2}\right), \quad (55)$$

and thus the exact boundary data can be easily derived by inserting Eqs. (52) and (53) into the above equation.

We have applied the new method to this example by fixing $R_0 = \rho_{\min} = 3$, $m = 20$ and $\alpha = 10^{-5}$. In Fig. 3 we compare the exact solution with numerical solution along a circle with radius 10. It can be seen that the numerical solution is almost coincident with the exact solution, of which the L^2 error is about 5.02×10^{-4} . Also we are imposed a random noise with intensity $\sigma = 0.003$ by

$$\hat{h}(\theta_i) = h(\theta_i)[1 + \sigma R(i)] \quad (56)$$

on the exact boundary data, of which the numerical solution was shown in the same figure by the dashed-dotted line. The new method is robust against the disturbance on the boundary data.

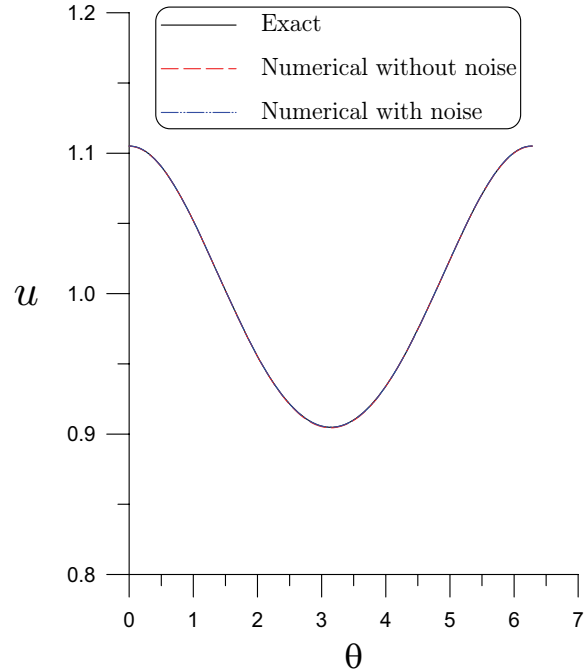


Figure 3: Comparing the exact solution and numerical solutions with and without noise for Example 2.

5.3 Example 3 (interior problem)

In this example we consider another epitrochoid boundary shape with $a = 4$ and $b = 1$; see Fig. 4. For this example we also investigate the condition number. When m increases the condition number also increases as shown in Fig. 5(a); however, even with $m = 30$ the condition number is still smaller than 100. The condition number increases with respect to R_0 as shown in Fig. 5(b), which indicates that for this case with $R_0 = \rho_{\max} = 6$ the condition number getting the smallest value.

The analytical solution is supposed to be

$$u(x,y) = x^2 - y^2, \quad (57)$$

and then the exact boundary data can be easily derived by inserting Eqs. (52) and (53) into the above equation.

In the numerical computation we have fixed $R_0 = \rho_{\max} = 6$, $m = 5$ and $\alpha = 10^{-15}$. In Fig. 4 we compare the contour levels of potential $u = -4$ and $u = 2$ for exact solutions and numerical solutions. It can be seen that the numerical results

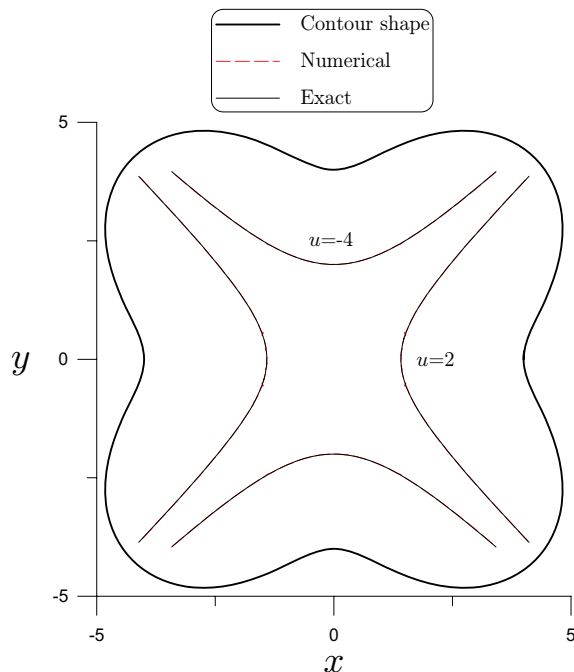


Figure 4: Comparing the exact and numerical contour levels of potential for Example 3.

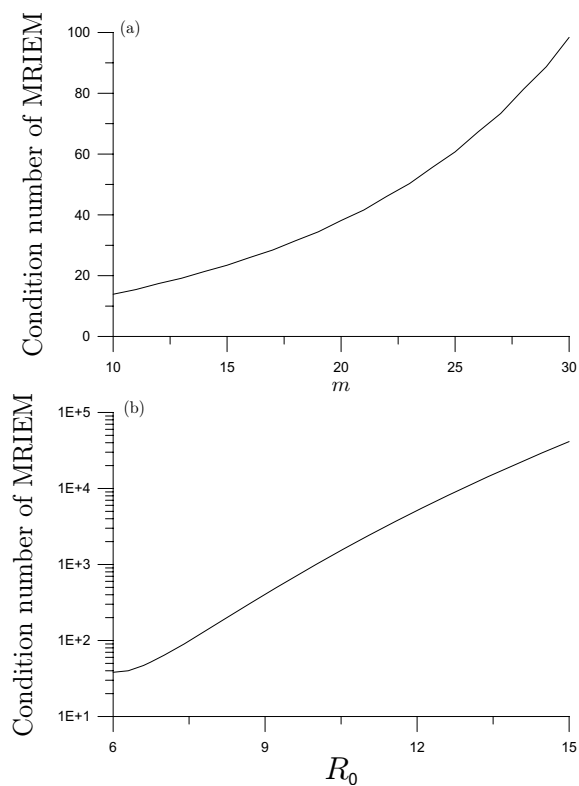


Figure 5: For Example 3 we plotting the condition number with respect to m in (a) and R_0 in (b).

are almost coincident with the exact ones. The accuracy of the numerical solutions are found to be good with the L^2 error about 1.36×10^{-13} .

5.4 Example 4 (interior problem)

For this example the solution domain is a simple disk with a radius equal to 2. To illustrate the accuracy and stability of the new method we consider the following analytical solution [Lesnic, Elliott and Ingham (1998); Jin (2004)]:

$$u(x,y) = \cos x \cosh y + \sin x \sinh y. \tag{58}$$

The exact boundary data can be easily derived by inserting $x = 2 \cos \theta$ and $y = 2 \sin \theta$ into the above equation.

In the numerical computation by using Eq. (47) we have fixed $R_0 = 2$, $m = 20$ and $\alpha = 10^{-6}$. In Fig. 6(a) we compare the exact solution with numerical solution along a circle with radius 1. It can be seen that the numerical solution is very close to the exact solution, of which the L^2 error is about 1.5×10^{-4} and the pointwise absolute error is plotted in Fig. 6(b). Also we are imposed a random noise with intensity 1% ($s = 1$) on the exact boundary data, of which the numerical solution was shown in the same figure by the dashed-dotted line. Even under a large noise the numerical error is still in the order of 10^{-3} . Therefore, we can say that the new method is robust against the disturbance.

6 Conclusions

In this paper we have proposed a new meshless method to calculate the solutions of Laplace equation in arbitrary interior or exterior plane domains. It was demonstrated that in a regularized sense we can find a semi-analytical solution of the boundary condition on an artificial circle, which requires only a few integrals on the circle. The numerical examples reveal that the effectiveness and the accuracy of the new method are fairly good. Even under a large noise on the boundary data, the numerical solutions are also stable and accurate without needing extra treatment. The robustness of the present method of

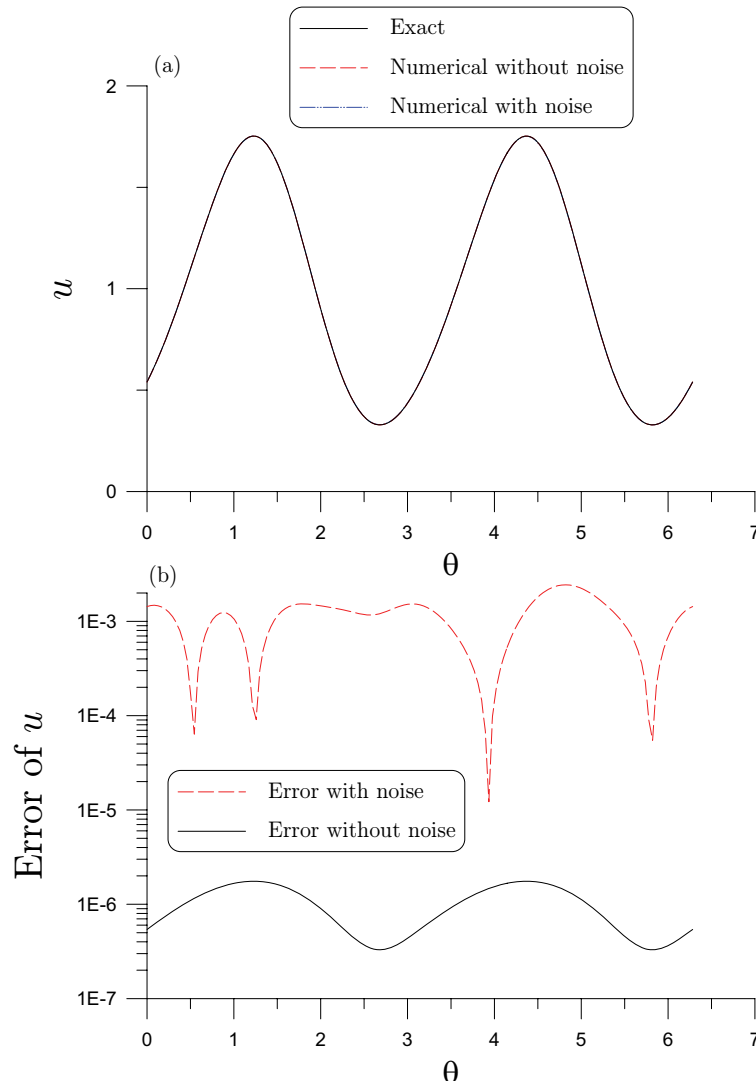


Figure 6: For Example 4 (a) comparing the exact solution and numerical solutions with and without noise, and (b) displaying the numerical errors.

MRIEM comes from the well-posedness of its linear equations system to determine the Fourier coefficients of unknown boundary function defined on an artificial circle. When directly using these Fourier coefficients in the solution of Laplace problem as shown by Eq. (44), the computational cost can be saved much, which only requires to solve a linear equations system with moderate dimension, and the condition number is very small as compared with the traditional Trefftz method and the method of fundamental solutions. Speaking conclusively, the new method of MRIEM possesses several advantages than the conventional boundary-type solution methods, includ-

ing mesh-free, singularity-free, non-illposedness, semi-analyticity, efficiency, accuracy and stability.

References

- Atkinson, K.** (1997): The Numerical Solution of Integral Equations of the Second Kind. Cambridge University, Cambridge, UK.
- Atluri, S. N.; Kim, H. G.; Cho, J. Y.** (1999): A critical assessment of the truly meshless local Petrov-Galerkin (MLPG), and local boundary integral equation (LBIE) methods. *Comp. Mech.*, vol. 24, pp. 348-372.

- Atluri, S. N.; Shen, S.** (2002): The meshless local Petrov-Galerkin (MLPG) method: a simple & less-costly alternative to the finite element and boundary element methods. *CMES: Computer Modeling in Engineering & Sciences*, vol. 3, pp. 11-51.
- Chen, J. T.; Lin, S. R.; Chen, K. H.** (2005): Degenerate scale problem when solving Laplace's equation by BEM and its treatment. *Int. J. Num. Meth. Engng.*, vol. 62, pp. 233-261.
- Chen, J. T.; Shen, W. C.; Chen, P. Y.** (2006): Analysis of circular torsion bar with circular holes using null-field approach. *CMES: Computer Modeling in Engineering & Sciences*, vol. 12, pp. 109-119.
- Chen, J. T.; Wu, C. S.; Lee, Y. T.; Chen, K. H.** (2007): On the equivalence of the Trefftz method and method of fundamental solutions for Laplace and biharmonic equations. *Comp. Math. Appl.*, in press.
- Huang, S. C.; Shaw, R. P.** (1995): The Trefftz method as an integral equation. *Adv. Engng. Software*, vol. 24, pp. 57-63.
- Jin, B.** (2004): A meshless method for the Laplace and biharmonic equations subjected to noisy boundary data. *CMES: Computer Modeling in Engineering & Sciences*, vol. 6, pp. 253-261.
- Kita, E.; Kamiya, N.** (1995): Trefftz method: an overview. *Adv. Engng. Software*, vol. 24, pp. 3-12.
- Kress, R.** (1989): *Linear Integral Equations*. Springer, Berlin.
- Lavrentiev, M. M.** (1967): *Some Improperly Posed Problems of Mathematical Physics*. Springer, New York.
- Lesnic, D.; Elliott, L.; Ingham, D. B.** (1998): The boundary element method solution of the Laplace and biharmonic equations to noisy boundary data. *Int. J. Num. Meth. Engng.*, vol. 43, pp. 479-492.
- Liu, C.-S.** (2007a): Elastic torsion bar with arbitrary cross-section using the Fredholm integral equations. *CMC: Computers, Materials & Continua*, vol. 5, pp. 31-42.
- Liu, C.-S.** (2007b): A highly accurate collocation Trefftz method for solving the Laplace equation in the doubly connected domains. *Numerical Methods for Partial Differential Equations*, in press.
- Liu, C.-S.** (2007c): A MRIEM for solving the Laplace equation in the doubly-connected domain. *CMES: Computer Modeling in Engineering & Sciences*, in press.
- Young, D. L.; Chen, K. H.; Lee, C. W.** (2005): Novel meshless method for solving the potential problems with arbitrary domain. *J. Comp. Phys.*, vol. 209, pp. 290-321.

